PHILOSOPHICAL TRANSACTIONS OF THE ROYAL SOCIETY B

Phil. Trans. R. Soc. B (2011) **366**, 1466–1476
doi:10.1098/rstb.2010.0316

Review

Skeletal muscle design to meet functional demands

Richard L. Lieber[1,*] **and Samuel R. Ward**[1,2]

[1]*Department of Orthopaedic Surgery, and* [2]*Department of Radiology, University of California San Diego, San Diego, CA 92121, USA*

Skeletal muscles are length- and velocity-sensitive force producers, constructed of a vast array of sarcomeres. Muscles come in a variety of sizes and shapes to accomplish a wide variety of tasks. How does muscle design match task performance? In this review, we outline muscle's basic properties and strategies that are used to produce movement. Several examples are provided, primarily for human muscles, in which skeletal muscle architecture and moment arms are tailored to a particular performance requirement. In addition, the concept that muscles may have a preferred sarcomere length operating range is also introduced. Taken together, the case is made that muscles can be fine-tuned to perform specific tasks that require actuators with a wide range of properties.

Keywords: skeletal muscle architecture; muscle design; sarcomere length

1. INTRODUCTION

Skeletal muscles are velocity- and length-dependent force producers. Because of this high velocity- and length-dependence, movement necessarily alters the force produced by a muscle and thus, the problem of placing muscles within the skeletal system is formidable. In this paper, we will review the basic mechanical properties of muscle, as well as muscle design, and use several examples from the animal kingdom to better understand the relationship between skeletal muscle design and performance.

2. MUSCLE MECHANICAL PROPERTIES

(a) *Isometric length–tension relationship*

One of the most fundamental properties of skeletal muscle is that the amount of force it generates depends on its length. This work was elucidated at the single fibre level in the classic studies by Gordon *et al.* [1,2]. In this relationship, skeletal muscle fibre force production is defined in terms of myofilament overlap, i.e. in terms of sarcomere length (figure 1*a*). At optimal length, where actin–myosin interactions are maximal, muscle generates maximum force (region 2 in figure 1*a*). As sarcomere length increases (region 3 in figure 1*a*), force decreases owing to the decreasing number of interactions between actin and myosin myofilaments. At lengths shorter than the optimum (region 1 in figure 1*a*), force decreases owing to double interdigitation of actin filaments with both myosin and actin filaments from opposite sides of the sarcomere. While this relationship has been challenged [3], to a first approximation, muscle force generation can be considered as a direct function of sarcomere length, and whole muscle force generation results from the aggregate force produced by all of the sarcomeres. Exceptions to this rule are likely to be small in magnitude and method-dependent.

While the sarcomere length–tension relationship can be considered a property of vertebrate skeletal muscle, it is not clear the extent to which this property is functionally meaningful *in vivo*. As an example of this point, consider the fact that there is good evidence in swimming fish, that sarcomere length remains more or less optimal [5,6]. Therefore, even though the sarcomere length–tension relationship can be experimentally measured in fish muscle [7], it may simply be a property of the muscle fibre itself that is never exploited *in vivo* since, *in vivo*, sarcomere length remains near the optimum. However, in other systems where sarcomere lengths have been measured, the change in muscle force with sarcomere length that occurs during joint rotation appears to be accommodated in the design of the system. One of those that we have studied in some detail, is the human wrist [8,9]. In this system, it was demonstrated that wrist extensor muscles operate at longer sarcomere lengths when compared with flexor muscles. In this way, as the wrist rotates from the flexed to the extended positions, torque remains balanced (see more detailed discussion below). For this case, it appears that the sarcomere length–tension relationship is actually exploited to create a mechanical design for wrist balance and stability.

While the active length–tension properties of skeletal muscle are consistent between sarcomeres, the passive length tension properties of muscle fibres and whole muscles are less consistent and less well understood. While it has been demonstrated that the giant elastic protein titin is a major load bearing structure in the vertebrate myofibril [10,11], it is not clear the extent to which titin-mediated forces are relevant in

* Author for correspondence (rlieber@ucsd.edu).

One contribution of 15 to a Theme Issue 'Integration of muscle function for producing and controlling movement'.

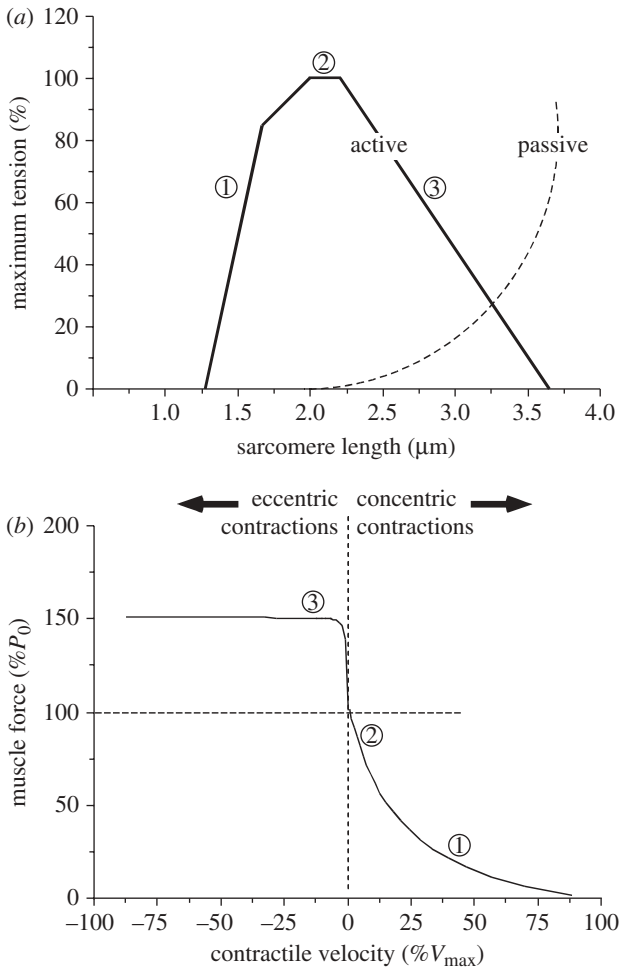

Figure 1. Basic biomechanical properties of skeletal muscle. (*a*) The isometric sarcomere length–tension curve defined for frog skeletal muscle obtained using sequential isometric contractions in single muscle fibres (solid line). Dotted line represents passive muscle tension borne by the muscle without activation. Numbers shown above the active curve represent the three main regions of the length–tension curve: the ascending limb (1), plateau (2) and descending limb (3). (*b*) The isotonic muscle force–velocity curve for skeletal muscle obtained using sequential isotonic contractions. The circled numbers represent the force and velocity data from two concentric contractions (1,2) and one eccentric contraction (3). Note that force increases dramatically upon forced muscle lengthening and drops precipitously upon muscle shortening. Figures modified from Lieber [4].

whole-muscle passive force production. For example, in a recent report in which titin molecular masses were measured in single muscle cells that were also mechanically tested, there was only a weak insignificant correlation between fibre passive elastic modulus and titin size [12].

(b) *Isotonic force–velocity relationship*

The force–velocity relationship in skeletal muscle describes the dependence of muscle force generation on contraction velocity. As muscles begin to shorten and sarcomere velocity changes from zero to a finite value, force drops, simply because the probability of interaction between actin and myosin decreases [13,14]. The decreased probability of cross-bridge interaction means that muscle force also decreases as a function of shortening velocity. The nature of the force decrease is nonlinear (figure 1*b*). In fact, the hyperbolic decrease in force with velocity suggests that muscles are not very effective at generating forces when shortening velocity is high. In terms of designing a muscle for a particular task, it would be disadvantageous to design a muscle to operate normally at high shortening velocities, since the relative force generated would be relatively low. There are several strategies used to ensure modest shortening velocities during movement—designing muscles with long fibres, placing them across multiple joints and activating them during lengthening (see below).

3. SKELETAL MUSCLE ARCHITECTURE

A number of anatomical and functional studies have been performed to determine structural factors that are the best predictors of muscle force and excursion. Clearly, muscle size impacts its functional properties, but it might be surprising to understand that muscle size (i.e. mass or volume) is not a very good predictor of muscle function. In fact, the structural property that best predicts a muscle's force-generating and moving capacity is its architecture. Skeletal muscle architecture is defined as the number and orientation of the muscle fibres within a muscle [15–17]. The classic textbooks distinguish between muscles that have fibres that span the length of the muscle (parallel architecture) in contrast to muscles containing shorter fibres that extend at an angle along the length of muscle (pennate or multi-pennate architecture; figure 2). Strictly speaking, a particular muscle may actually have a structure that is a combination of these architectural strategies but will have a tendency towards one particular type of architecture. Additionally, while there is a great deal of variability in muscle architecture between muscles within an individual, there is consistent architectural design within muscles among individuals. This can be seen by the fact that published between-individual variability is relatively small within the hindlimbs of a given species [17–25].

The most important architectural parameter is fibre length within a muscle. This is because muscle fibre length permits greater excursion of a particular muscle as well as a muscle's 'packing' strategy. The length–tension curve and the force–velocity curves appear to scale nicely with muscle fibre length in most skeletal muscles—the length–tension curve gets 'wider' with increasing fibre length and the force–velocity curve has an increased maximum velocity. Experimental evidence supporting this assertion comes from isotonic experiments on cat semitendinosus muscles [26] and isometric experiments on relatively large rabbit muscles (figure 3) [27]. The explanation for the relationship between muscle fibre length and excursion is based on the concept that greater serial sarcomere number (i.e. greater fibre length) leads directly to a greater muscle excursion because the excursions of the individual sarcomeres in series are additive. A particularly convincing demonstration of the idea that the whole muscle length–tension curve

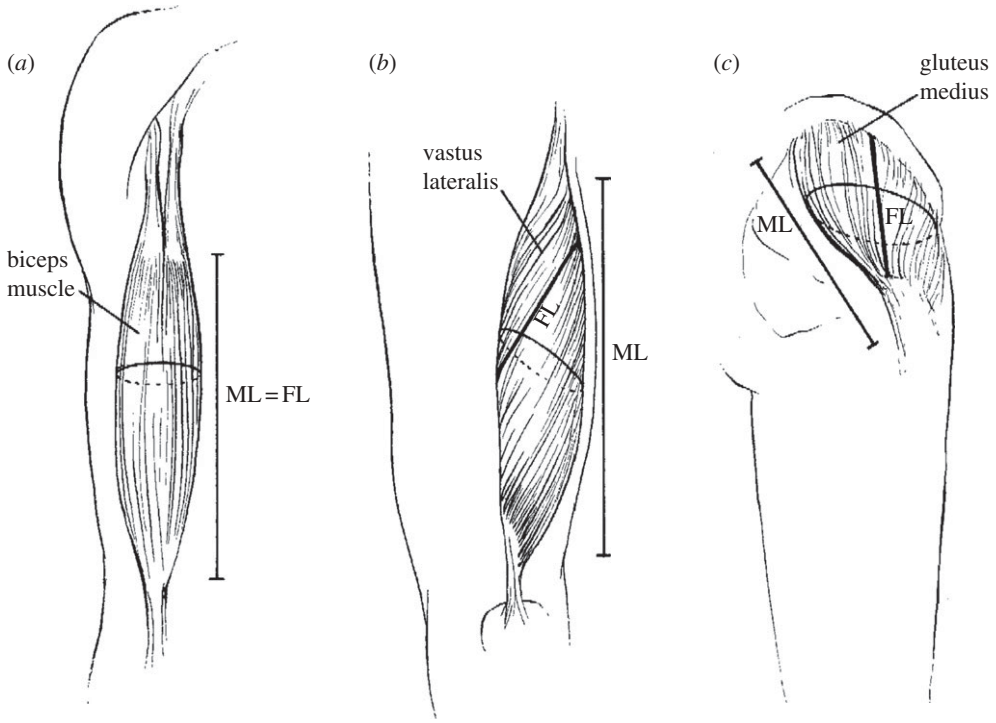

Figure 2. Generalized picture of muscle architectural types. Skeletal muscle fibres may be oriented parallel to the muscle's force-generating axis (*a*; known as 'longitudinal' architecture), at a fixed angle relative to the force-generating axis (*b*; known as 'pennate' architecture), or at multiple angles relative to the force-generating axis (*c*; known as 'multi-pennate' architecture). Each of these drawings represents an idealized view of muscle architecture and probably does not adequately describe any single muscle. (ML, muscle length; FL, fibre length.) Figure modified from Lieber [4].

is simply scaled from sarcomere properties comes from isometric contractile studies of a mouse in which the nebulin gene is knocked out [28]. Nebulin is believed to affect thin filament length and the nebulin knockout mouse has sarcomeres with reduced length. It is predicted that the decreased filament length would result in an isometric length–tension curve with a decreased optimal length and a narrower width. Recent experimental measurements of the whole muscle isometric length–tension curve generated data in agreement with this prediction [29].

The magnitude of isometric force generation is determined by the number and arrangement of muscle fibres within the muscle. Unfortunately, it is very difficult to quantify either muscle fibre number or the precise fibre arrangement within a muscle. This is because muscle fibres need not run the entire length of the muscle, and they may be oriented at an angle relative to the muscle's axis. As a result of this difficulty, the total cross-sectional area of the muscle fibres is approximated mathematically, by the so-called physiological cross-sectional area (PCSA) term, which is calculated using the following equation:

$$\mathrm{PCSA}(\mathrm{cm}^2) = \frac{\text{muscle mass (g)} \cdot \cos\theta}{\rho(\mathrm{g\,cm}^{-3}) \cdot \text{fibre length (cm)}}, \qquad (3.1)$$

where ρ represents muscle density ($1.05\ \mathrm{g\,cm}^{-3}$ for fixed mammalian muscle) [30] and θ represents surface pennation angle. Inspection of this equation (see discussion in [31]) reveals that PCSA area may not actually represent any actual anatomical cross-sectional area. One study performed in the guinea pig hindlimb showed that PCSA is proportional to isometric force capacity, with a conversion factor of $22.5\ \mathrm{N\,cm}^{-2}$ (approx. 250 kPa). Thus, to a first approximation it is possible to estimate the maximum isometric force a muscle can generate by multiplying its PCSA by $22.5\ \mathrm{N\,cm}^{-2}$. Note that other values have been used in the literature without necessarily being experimentally verified [32,33]. There are no high-resolution experimental data from mammalian muscle that values other than $22.5\ \mathrm{N\,cm}^{-2}$ are possible in normal mammalian muscles.

4. EXAMPLES OF HUMAN MUSCLE ARCHITECTURE

While the theoretical concept of muscle architecture is relatively straightforward, actually measuring it is fairly difficult. Numerous studies performed in humans and in animals (see references above) have defined architectural properties by performing microdissection of small fibres and fibre bundles from a variety of muscles throughout the limb. For the purposes of this review, we will simply present the lower extremity of humans as an example, but it should be noted that a number of comparative architectural studies have also been performed that can provide insight into animal design. In the human lower extremity, the three strongest muscles (based on PCSA) are the soleus, vastus lateralis and gluteus medius (figure 4). This may not be surprising as they are all antigravity muscles; but it is surprising that the single strongest muscle is observed distally in the leg where muscle volumes tend to be smallest and even though the mass of the soleus is not the greatest muscle mass in the leg.

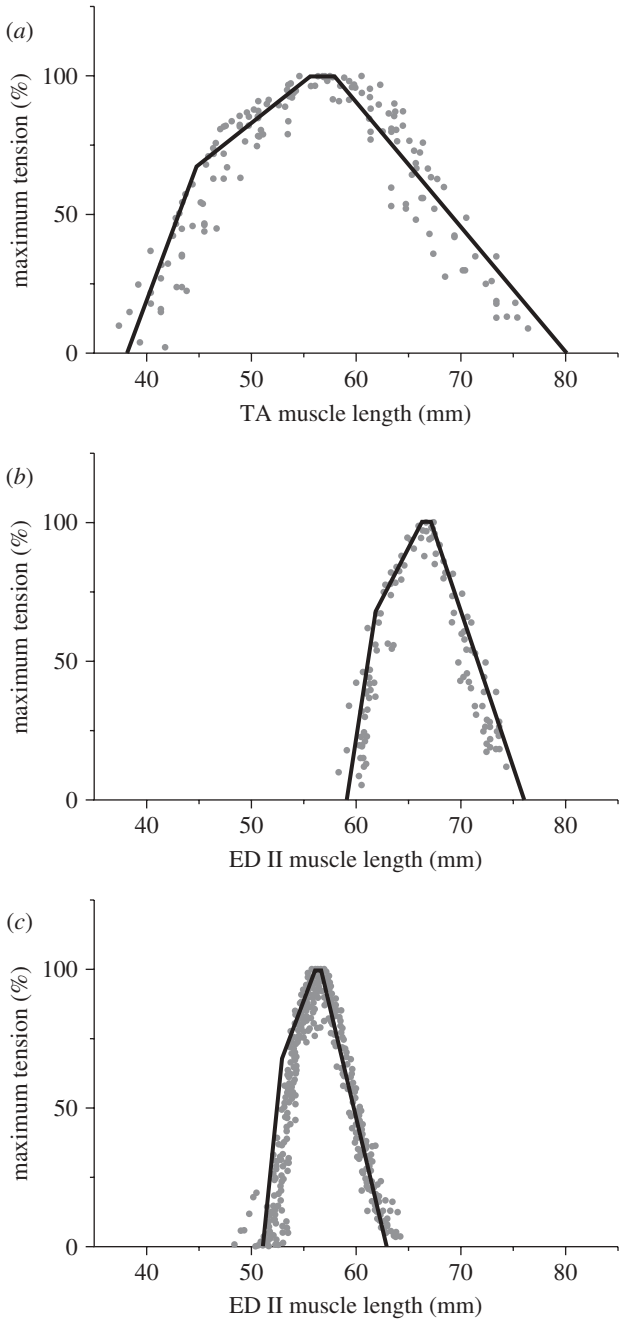

Figure 3. Skeletal muscle length–tension properties are well-approximated by the length–tension relationship. The active theoretical length–tension curve (black line) and experimental (grey circles) muscle length–tension relation are shown for three rabbit muscles of different architectures: (*a*) TA, tibialis anterior; (*b*) EDL, extensor digitorum longus; (*c*) ED II, second toe digital extensor. Theoretical and experimental data were highly correlated for all muscles (TA: $r^2 = 0.81$, intraclass correlation coefficient: ICC = 0.84; EDL: $r^2 = 0.90$, ICC = 0.86; ED II: $r^2 = 0.87$, ICC = 0.89). Relative tension (muscle tension normalized to maximum tension) was plotted on the ordinate to facilitate comparison between muscles. Data replotted from Winters *et al.* [27].

This emphasizes the fact that the human soleus represents an extreme in terms of architectural design. Leg muscles with the longest fibre lengths (implying the greatest excursion) are the sartorius, gracilis and semitendinosus (figure 4). Although they all cross the hip and knee, the feature they share in common is knee flexion. The semitendinosus ranks high in fibre length only when the proximal and distal heads of the muscle are added in series, which probably reflects its actual physiological function based on its dual innervation [26].

When human leg muscle groups that cross a common joint are compared, the ankle plantarflexors have larger total PCSAs and shorter mean fibre lengths compared with dorsiflexors. Knee extensors have larger total PCSAs compared with knee flexors, but both groups have similar fibre lengths (figure 4). Hip extensors have larger total PCSAs compared with the flexors, abductors and adductors, and the extensors and abductors have shorter mean fibre lengths than flexors and adductors (figure 4).

In terms of fundamental design features of individual muscles, large mass and short fibre length both contribute to large PCSA when the lower extremity is considered as a whole. For example, as mentioned above, the soleus muscle has a modest mass (275 g) combined with very short fibres (4 cm), which results in its exceptionally large PCSA. This is in comparison with the vastus lateralis, which has an almost 50 per cent greater mass (376 g) but a modest fibre length (10 cm) which results in a smaller PCSA.

5. NON-INVASIVE MEASUREMENT OF ARCHITECTURAL PROPERTIES

It is possible to estimate muscle architectural properties non-invasively using imaging methods. The most popular method currently in use is ultrasound [35]. Ultrasound is relatively inexpensive, has relatively high temporal resolution, provides a vivid image of the muscle and presents little if any risk to the patient. (figure 5) The two main limitations of ultrasound are (i) the spatial resolution cannot quite resolve muscle fibres, and (ii) there is no estimate sarcomere length and, therefore, fascicle lengths that are measured by ultrasound are not uniquely related to force-generating properties. Another way of saying this is, it is not clear whether long fascicles represent an average fibre length that is highly stretched or if the long fascicles really represent a large number of serial sarcomeres. Thus, typically, muscle ultrasound measurements are performed and then literature sarcomere length values are used to try to perform some type of normalization. This is not without experimental risk because it is not possible in most cases to know any sarcomere length that corresponds to any particular joint angle.

A second method used to non-invasively image muscle architecture is Magnetic Resonance Imaging (MRI). MRI has an advantage over ultrasound by having much higher spatial resolution (tens of microns), being able to perform large-scale three-dimensional reconstructions, and even being able to resolve whole fascicle dimensions. However, as with ultrasound, an MR image does not provide any insight into sarcomere length or serial sarcomere number. A typical MR image is shown in figure 6 where it can be seen that this particular muscle was serially imaged in the axial plane (figure 6*a*) and then 'segmented' (i.e. structurally isolated from surrounding tissues), reconstructed (figure 6*c*,*d*) and compared

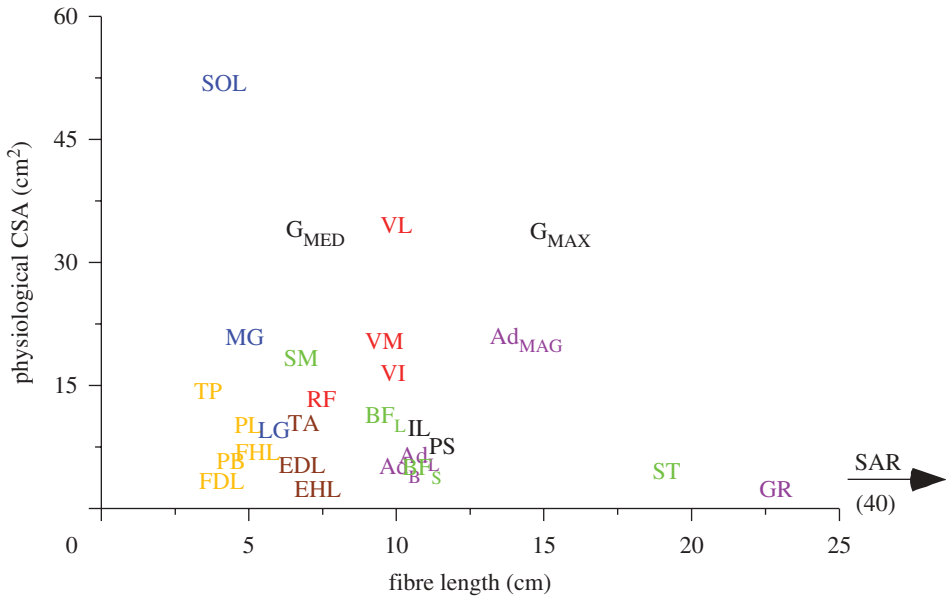

Figure 4. Scatter graph of fibre length and physiological cross-sectional areas (PCSAs) of muscles in the human lower limb. Fibre length is proportional to muscle excursion while PCSA is proportional to maximum muscle force. Thus, this graph can be used to compare the relative forces and excursions of leg muscles. Similar colours are used for the same functional groups. Data from Ward *et al.* [34]. (Ad_B, adductor brevis; Ad_L, adductor longus; AM, adductor magnus; BF_L, biceps femoris, long head; BF_S, biceps femoris, short head; EDL, extensor digitorum longus; EHL, extensor hallucis longus; FDL, flexor digitorum longus; G_{MAX}, gluteus maximus; G_{MED}, gluteus medius; GR, gracilis; FHL, flexor hallucis longus; IL_{PS}, iliopsoas; LG, lateral gastrocnemius; MG, medial gastrocnemius; PEC, pectineus; PB, peroneus brevis; PL, peroneus longus; RF, rectus femoris; SAR, sartorius; SM, semimembranosus; SOL, soleus; ST, semitendinosus; TA, tibialis anterior; TP, tibialis posterior; VI, vastus intermedius; VL, vastus lateralis; VM, vastus medialis.)

with an actual dissected specimen (figure 6*e*). While this approach simply reconstructs the muscle volume, an exciting future imaging possibility is the use of diffusion tensor-MRI and fibre tract mapping that can provide insight into muscle fibre orientation. This type of imaging may ultimately be able to define some of the very complex orientations of fibres within the entire muscle without laboriously microdissecting small bundles from the tissue [37,38]. (It should be noted that this approach still does not yield sarcomere length.) A final approach used to investigate *in vivo* muscle architecture is to measure sarcomere length directly by laser diffraction [39] or two-photon microscopy [40]. Both of these methods are invasive, in that the muscle must be directly impaled. Laser diffraction has the advantage of being relatively simple to use intraoperatively with a relatively low-power hand-held laser device. Two-photon microscopy has the advantage of being able to be used transcutaneously and provides separate two-dimensional sarcomere orientation within an illuminated region. Without question, both methods will be developed further over the coming years. Their power is that, by combining sarcomere length with architectural parameters, relatively high-resolution mathematical models of joint function can be created (see examples in [33,41]).

6. INTEGRATING MUSCLES WITH MOVEMENT

It is difficult to design a muscle to perform a certain task, based largely on the general muscle mechanical properties described above. Previously, it was highlighted that muscles are relatively length- and velocity-sensitive. Thus, muscles that must shorten at high velocities necessarily require a design that allows them to do so without losing much force. How does one design these types of muscles given the volume (mass) constraints of a limb?

This idea of serial versus radial mass distribution is illustrated in the series of graphs in figure 7. Overall, the figure illustrates the theoretical relationship that occurs between muscle fibre length and force for a muscle with constant mass. This is a thought experiment designed to demonstrate that, as sarcomeres are preferentially arranged in series or in parallel (and muscle mass remains constant) force changes simply owing to the fibre architectural features. For example, if one considers the relationship between fibre length and isometric force production given constant mass, as fibre length increases, isometric force production decreases nonlinearly (figure 7*a*) because increasing fibre length places more sarcomeres in series and there are fewer fibres in the muscle itself. One might ask, 'Why isn't it a good idea to make a muscle with more short fibres, to make isometric force higher?' This point is addressed in figure 7*b* where it can be seen that for a given shortening velocity (and again, constant mass) as fibre length increases dynamic force also increases nonlinearly. This occurs because the longer the fibre for a given shortening velocity, the lower is the sarcomere velocity, and thus, the lower the relative shortening velocity on force–velocity curve. These two effects of fibre length on isometric and dynamic force oppose one another. Therefore, for muscles that are required to function

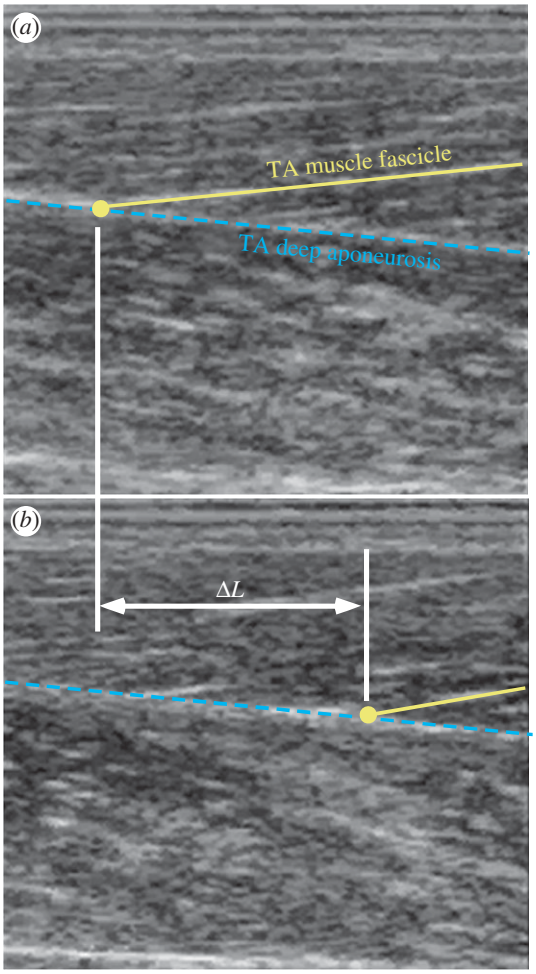

Figure 5. Ultrasonic measurement of muscle fibre shortening and tendon lengthening during 'isometric' dorsiflexion of the tibialis anterior. (*a*) Sagittal plane image of anterior compartment prior to contraction. (*b*) Sagittal plane image of anterior compartment during contraction. Note the shift in an individual muscle fascicle that is followed in the image during this process and the change in length (ΔL) and pennation angle calculated. Data from Ito *et al.* [36]. Images courtesy of Dr Yasuo Kawakami, Waseda University, Japan.

more or less isometrically, a design bias towards short fibres would be expected, while muscles that are designed to shorten at relatively high velocities would have a design bias towards long fibres. This thought experiment was tested for a specific mouse dorsiflexor muscle (the numbers in figure 7 actually refer to that muscle). Interestingly, if one combines the isometric force potential and dynamic force potential of that muscle, an optimal fibre length is predicted at the peak of the force–fibre length relationship (figure 7*c*). For the case of the mouse dorsiflexor that optimal fibre length was predicted to be 8.1 mm while the actual observed fibre length from these animals was very close to that, measured as 7.6 ± 0.2 mm [42]. Therefore, one muscle design strategy appears to be to adjust fibre length (or architecture) in order to maximize force production for a given muscle under its functional conditions.

A second strategy to optimize muscle design for a particular task is for muscles to cross multiple joints. During normal gait, biarticular muscles are often activated and, interestingly, rotation at one joint tends to shorten the muscle while rotation at another joint tends to lengthen the same muscle. Therefore, by placing muscles across multiple joints, fibre length can remain more or less isometric during normal movement. By preventing high shortening velocities, higher forces are produced. An example of this is the hamstring muscles that are used during normal walking, as hip extensors and knee flexors. Since hip and knee extension often occur simultaneously, the net result during movement is that the hamstring has a smaller length change compared with the situation where two separate monoarticular muscles would be used to control the hip and the knee [43]. In fact, it gets even a little bit more complicated since biarticular muscles can also transfer moments from one joint to distal joints that they do not even cross by combining activation strategies with other muscles that cross common joints. This is one of the reasons that it can be very difficult to ascribe a specific role to a specific muscle during gait.

7. DESIGN PARAMETERS OF MUSCLE-JOINT SYSTEMS

(a) *Fibre length : moment arm ratio*

Interactions between muscles and joints occur during movement. While muscle properties are very important, it is the relative length change in the muscle for a given amount of joint rotation that most affects function. A relevant relationship between these muscle properties and skeletal dimensions can be defined by calculating the fibre length-to-moment arm ratio. This ratio represents a muscle's sensitivity at the sarcomere level to joint rotation, and has been shown to vary widely within an organism, clearly reflecting the diverse functions of various musculoskeletal systems [44]. An explicit demonstration of how fibre length-to-moment arm ratio can differ between two human wrist extensor muscles was reported based on measurements performed on surgical patients [45]. This comparison was made by directly measuring the relationship between sarcomere length and joint angle during hand surgery. The slope of the sarcomere length–joint angle curve provides an estimate of the fibre length-to-moment arm ratio—and will provide an estimate of the degree to which joint rotation affects force production. For all seven subjects studied, the slope of the sarcomere length–joint angle curve (i.e. $dSL/d\phi$) was greater for the extensor carpi radialis brevis (ECRB) muscle when compared with the extensor carpi radialis longus (ECRL). A relatively large degree of variability in $dSL/d\phi$ was observed between subjects for both the ECRB and ECRL (figure 8*a*). However, across all subjects, average $dSL/d\phi$ for ECRB was 9.06 nm deg^{-1} while that of the ECRL was about half of this value, or 4.69 nm deg^{-1}. We computed the ratio of $dSL/d\phi$ between the ECRB and ECRL within each subject and averaged these values across subjects. This average $dSL/d\phi$ ratio for the intraoperative sarcomere length data was 2.45 which was very close to the theoretical ratio of 2.42 that would be predicted based on muscle architecture [47] and wrist joint moment arms [48].

Thus, the ECRB and ECRL have relatively different architectural designs and these differences are actually

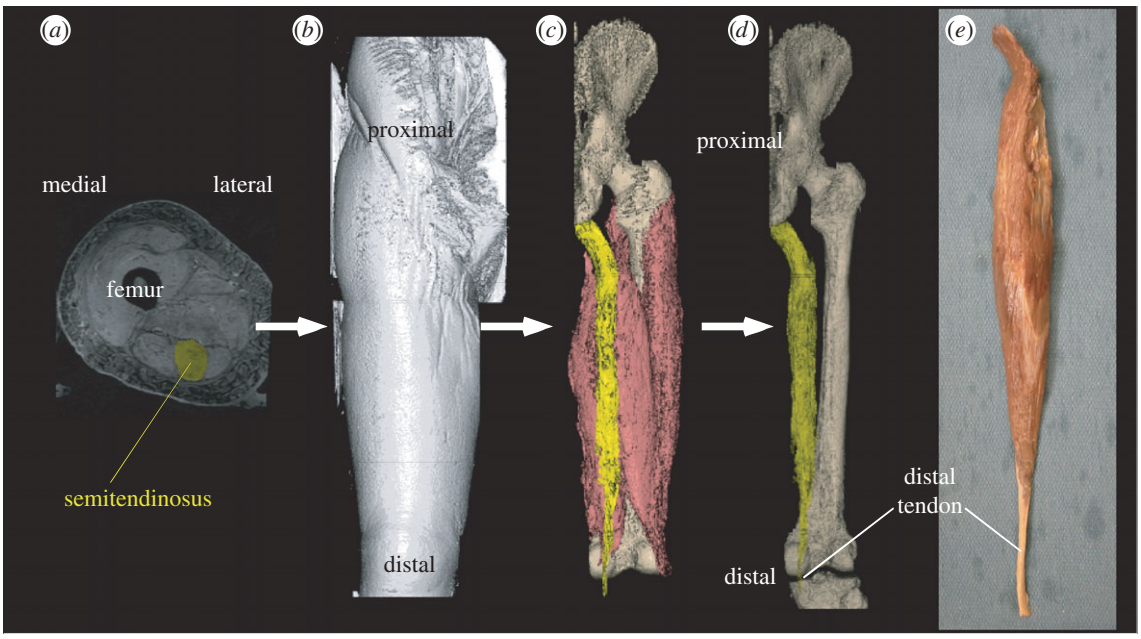

Figure 6. Magnetic resonance imaging (MRI) used to render and calculate muscle volume for a human semitendinosus (ST). (*a*) Serial contiguous slices are acquired in the transverse plane. ST is highlighted in yellow. (*b*) Serial images are registered to reconstruct the entire thigh. (*c*) Muscles are distinguished from other tissues to calculate total muscle volume. (*d*) ST muscle is isolated from the entire thigh and the PCSA calculated. (*e*) Comparative photograph of dissected human ST.

exacerbated by their different wrist moment arms. From a design point of view, a high moment arm : fibre length ratio results in a torque motor in which large fibre length changes produce large force changes during joint rotation and, thus, this motor would vary its torque output to as great an extent as the joint rotated. This approximates the design of the ECRB torque motor for wrist extension motions, based on its relatively short fibres and large moment arm. By contrast, the significantly longer fibres and smaller moment arm of the ECRL result in a torque motor with different functional properties. The ECRL-based motor retains a more constant torque output with joint rotation since, for a given amount of joint rotation, sarcomere length changes less.

Dynamically, the situation may be more complex as the architectural design that favours isometric force production may be disadvantageous in the dynamic situation as described above. For example, the ECRB has a higher predicted maximum isometric tension than the ECRL [47] because of its greater number of short muscle fibres. Yet, since these fibres are shorter, for a given angular velocity, force relative to maximum isometric tension decreases to a greater extent in the ECRB compared with the ECRL (figure 8*b*). Using the architectural properties of the two muscles, along with nominal values for the maximum contraction velocity (V_{max}) of mammalian muscle [49], the force–velocity relationship for each muscle can be determined. The exact values for V_{max} and the force–velocity curvature are not important in making this comparison as long as the ECRB and ECRL fibre-type distributions are not dramatically different from one another. The contraction velocity at which the ECRL becomes stronger is approximately 80 mm s^{-1} which, on the basis of the two muscle moment arms, corresponds to an angular velocity of approximately 240° s^{-1} (figure 8*b*). This results in a design in which the ECRB is stronger isometrically but, as angular velocity increases, the ECRL becomes the stronger muscle.

This differential muscle strength that is velocity-dependent may provide insight into the utility of having a diversity of design between these two muscles. The ECRB and ECRL muscles as a synergistic group produce a maximum tetanic tension of 25.6 kg and a V_{max} of approximately 2800° s^{-1}. In order for a single muscle to generate the same force while maintaining such a high V_{max}, the fibre length would have to be 76 mm (as for the ECRL to maintain the same V_{max}) and the cross-sectional area would have to be about 4.2 cm^2 (the sum of the two muscles' PCSAs to maintain the same maximum force). Using the simple equation for muscle PCSA [17] this single muscle would weigh 33.7 g, which is over 30 per cent greater than the sum of the two muscle masses. Having two muscles as synergists thus accomplishes the same task at the velocity extremes but with a lower mass and thus a lower metabolic cost and a lower moment of inertia.

(b) *Sarcomere length operating range*

Based on data from the wrist muscle and joint, it was calculated that wrist extensors are predicted to operate primarily on the plateau and descending limb of their sarcomere length–tension curve (figure 9) with all muscles generating maximal force in full extension. Only the ECRB was predicted to operate at sarcomere lengths corresponding to less than 80 per cent P_o in the normal range of motion. Wrist flexors were predicted to operate predominantly on the shallow and steep ascending limbs of their length–tension curve with both flexors generating maximal force in full wrist

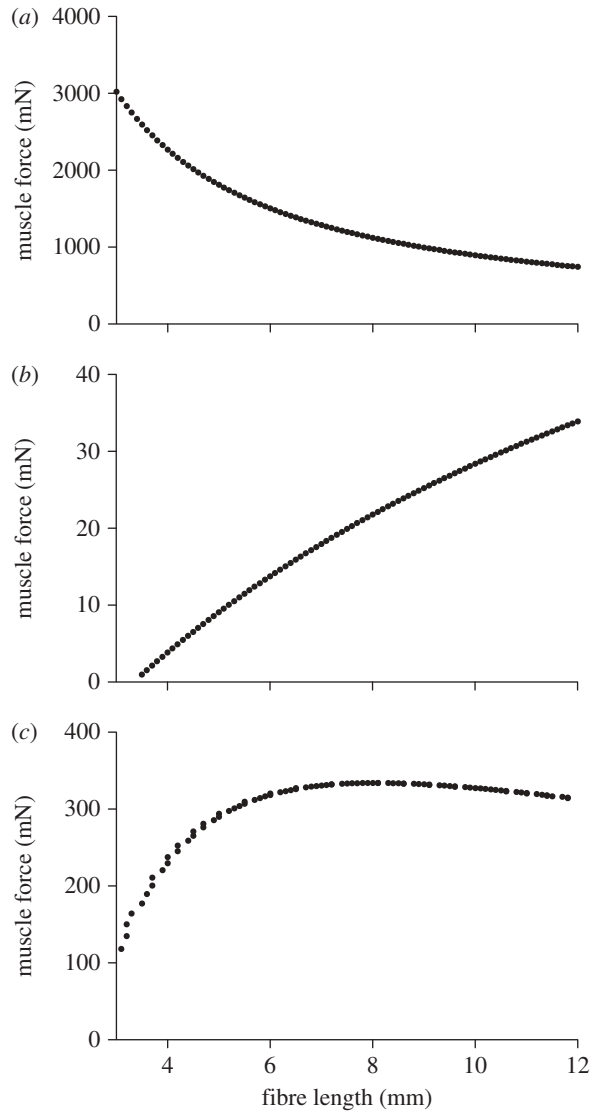

Figure 7. (*a*) Theoretical relationship between muscle fibre length and isometric force for a muscle with constant mass. (*b*) Theoretical relationship between muscle fibre length and dynamic muscle force for a muscle shortening at a constant velocity. (*c*) Tension calculated as fibre length is altered based on the isometric and isotonic effects shown in (*a*) and (*b*). Optimal fibre length results from a tradeoff between decreasing sarcomere shortening velocity (which increases force) and decreasing muscle isometric force capacity as fibre length increases. Data replotted from Lieber [42].

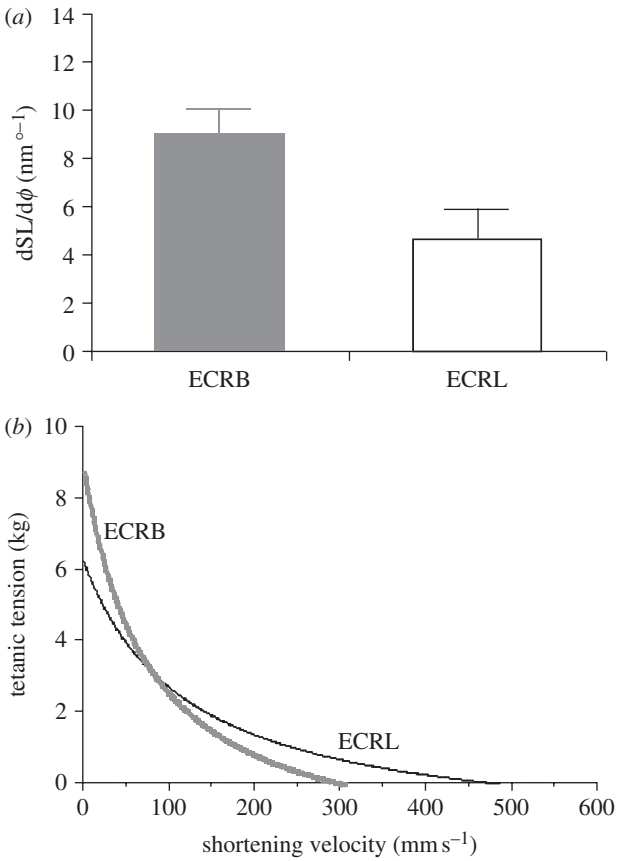

Figure 8. (*a*) Change in sarcomere length with changing wrist joint angle (dSL/dϕ) for the extensor carpi radialis brevis (ECRB) and extensor carpi radialis longus (ECRL) muscles. Values are actually calculated directly from intraoperative sarcomere length values measured during hand surgery. (*b*) Calculated force–velocity relationships for the ECRB and ECRL muscles based on muscle architecture and wrist joint moment arms. The two curves cross at an angular velocity of approximately 240° s^{-1} which, on the basis of the muscle moment arms, corresponds to a muscle velocity of approximately 80 mm s^{-1}. These data demonstrate that architectural 'design' can be used to favour isometric or isotonic force production and that synergists often have distinct architectural properties. Data from Lieber *et al.* [46].

extension (figure 9). Note that in full flexion, it is possible for wrist flexors to generate forces that are less than 50 per cent P_o.

Such a design presents interesting implications for the design of the wrist as a torque motor. Both flexor and extensor muscle groups generate maximum force with the wrist fully extended. As the wrist extends, maximum isometric extensor force increases owing to extensor shortening-up the descending limb of the length–tension curve and maximum isometric flexor force increases owing to flexor lengthening-up the ascending limb of the length–tension curve. This effect is superimposed upon an increasing extensor moment arm as the extensor muscles elevate off of the wrist under the extensor retinaculum and a decreasing flexor moment arm as the flexors juxtapose the wrist from the flexor retinaculum. Combining both muscles and joint effects, extensor muscle force is amplified by an increasing extensor moment arm while flexor muscle force is attenuated by the decreasing flexor moment arm. Importantly, since the flexors as a group develop significantly greater force that the extensors (owing to their larger PCSA), the net result is a nearly constant ratio of flexor to extensor torque over the wrist range of motion. In fact, while at the muscle level, the flexors are considerably stronger than the extensors [47,50], when including the wrist kinematics, extensor moment can actually exceed flexor moment. Additionally, wrist resistance to angular perturbation increases as the wrist is moved to full extension since both flexor and extensor moments increase in a similar fashion. Since this type of invasive sarcomere length measurement is rare, it is difficult to determine the extent to which this design principle applies to any other human musculoskeletal system. However, it is of interest to know that, in the cases where sarcomere

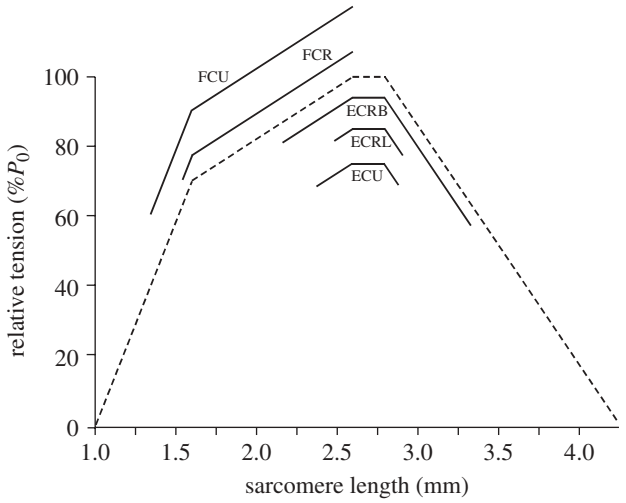

Figure 9. Operating ranges of the wrist motors on the isometric sarcomere length–tension relation. Note that wrist extensors operated primarily on the plateau region while the flexors operated predominantly along the ascending and steep ascending limbs. (Data are presented for flexion-extension in neutral forearm rotation.) Data from Loren & Lieber [48]. (FCU, flexor carpi ulnaris; FCR, flexor carpi radialis; ECRB, extensor carpi radialis brevis; ECRL, extensor carpi radialis longus; ECU, extensor carpi ulnaris.)

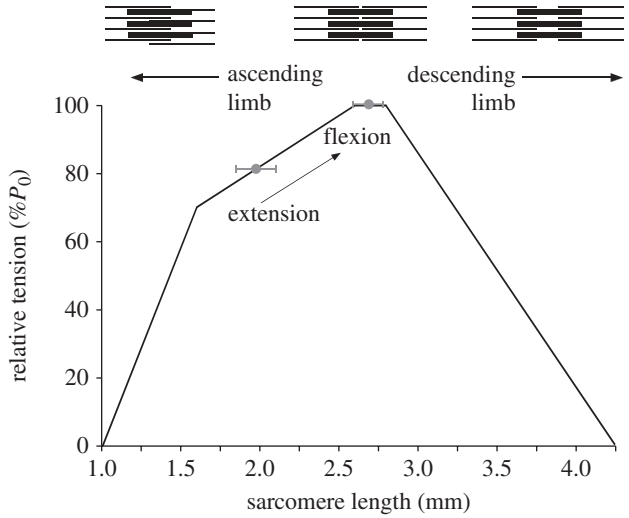

Figure 10. Sarcomere length operating range of the human multifidus muscle plotted on the human skeletal muscle sarcomere length tension curve (black line). Grey circles represent average sarcomere length obtained via biopsy in lumbar extension ($n = 8$) or lumbar flexion ($n = 5$), as reported by Ward *et al.* [51]. These data demonstrate that the multifidus muscle operates on the ascending limb of the length tension curve and becomes intrinsically stronger as the spine in flexed (arrow). Schematic sarcomeres are shown on the ascending and descending limb to scale, based on the quantification of actin and myosin filament lengths reported previously in Lieber *et al.* [39].

length has been measured, muscles tend to operate at extreme lengths rather than moderate lengths. Another clear example of this was recently observed for the tremendously strong multifidus muscle—a deep lumbar spine extensor [51]. Unlike the wrist muscles described above, the multifidus muscle remains on the ascending portion of its length–tension curve as the spine flexes (figure 10). This allows the multifidus muscle to become intrinsically stronger as the spine flexes until it would theoretically produce maximum force. This design is especially appealing as it creates a 'proportional feedback' system in which the greater the deflection from neutral, the greater the restoring force. Clinically, this provides the necessary stabilizing force as the body leans forward, a position known to elevate intradiscal pressure and cause increased low back pain in patients with spinal disorders. Secondarily, the data also demonstrate that the muscle does not lengthen sufficiently to operate onto the descending portion of the length tension curve, which would impair force production. Given this design feature, one could hypothesize that if the muscle operated at longer lengths, stability would be compromised. Whether chronic changes in sarcomere length operating range could result from disc disease, deformity, chronic disuse or surgical trauma is not yet known. However, these potential explanations for dysfunction are intriguing.

8. LIMITATIONS OF PRIMARY EXPERIMENTAL DATA

One of the most difficult aspects of trying to understand the *in vivo* design of skeletal muscle is obtaining primary experimental data from living animals and humans. Of course, the experiments most directly applicable to humans are performed on primates that greatly limit the ability to perform invasive studies. We and others have elected to study human muscle by studying orthopaedic surgery patients (who are already undergoing procedures), which permits measurement of both *in vivo* muscle and tendon parameters and obtaining biopsies. Others have addressed the movement question in animal models by implanting force transducers, either the buckle-type tendon force transducer [52,53], EMG-detecting electrodes in muscles [54] or length-measuring sonomicrometer crystals [55,56]. These are extremely elegant approaches that can provide extremely valuable information but are technically challenging. Finally, as a way to understand *in vivo* muscle function, modelling approaches have been undertaken. These approaches essentially treat the muscle, the tendons and the joint as modules with properties that are known, and the modules are assembled according to a conceptual framework [57]. This latter modelling approach is very powerful, in that global design strategies for entire organisms can be elucidated. Such approaches have already been performed in humans and animals [33,41,58]. However, because of the number of degrees of freedom in these models, the muscle properties themselves are fairly generic and it is not clear the extent to which design parameters can become apparent from such generic models. This must be the subject of future studies.

9. CONCLUDING REMARKS

Skeletal muscle mechanical properties are well-understood and present a challenge for 'designing' motors that function well in the context of movement.

However, we have seen that many muscles and joints have properties that suit them well to accomplish a particular task. In addition, these properties can be made complementary and even specific to a function. Future studies are required to understand the factors that allow these well-defined properties to develop in the first place and the extent to which they can be altered by surgical intervention or rehabilitative strategies.

REFERENCES

1 Gordon, A. M., Huxley, A. F. & Julian, F. J. 1966 The variation in isometric tension with sarcomere length in vertebrate muscle fibres. *J. Physiol. Lond.* **184**, 170–192.
2 Gordon, A. M., Huxley, A. F. & Julian, F. J. 1966 Tension development in highly stretched vertebrate muscle fibres. *J. Physiol. Lond.* **184**, 143–169.
3 Pollack, G. H. 1983 The cross-bridge theory. *Physiol. Rev.* **63**, 1049–1113.
4 Lieber, R. 2010 *Skeletal muscle structure, function, and plasticity*, 3rd edn. Philadelphia, PA: Lippincott Williams & Wilkins.
5 Lieber, R. L., Raab, R., Kashin, S. & Edgerton, V. R. 1992 Sarcomere length changes during fish swimming. *J. Exp. Biol.* **169**, 251–254.
6 Rome, L. C. & Sosnicki, A. A. 1991 Myofilament overlap in swimming carp. II. Sarcomere length changes during swimming. *Am. J. Physiol.* **163**, 281–295.
7 Granzier, H. L., Akster, H. A. & Ter Keurs, H. E. 1991 Effect of thin filament length on the force-sarcomere length relation of skeletal muscle. *Am. J. Physiol.* **260**, C1060–C1070.
8 Loren, G. J., Shoemaker, S. D., Burkholder, T. J., Jacobson, M. D., Fridén, J. & Lieber, R. L. 1996 Human wrist motors: biomechanical design and application to tendon transfers. *J. Biomech.* **29**, 331–342. (doi:10.1016/0021-9290(95)00055-0)
9 Lieber, R. L. & Friden, J. 1998 Musculoskeletal balance of the human wrist elucidated using intraoperative laser diffraction. *J. Electromyogr. Kinesiol.* **8**, 93–100. (doi:10.1016/S1050-6411(97)00025-4)
10 Labeit, S. & Kolmerer, B. 1995 Titins: giant proteins in charge of muscle ultrastructure and elasticity. *Science* **270**, 293–296. (doi:10.1126/science.270.5234.293)
11 Magid, A. & Law, D. J. 1985 Myofibrils bear most of the resting tension in frog skeletal muscle. *Science* **230**, 1280–1282. (doi:10.1126/science.4071053)
12 Ward, S. R., Tomiya, A., Regev, G. J., Thacker, B. E., Benzl, R. C., Kim, C. W. & Lieber, R. L. 2009 Passive mechanical properties of the lumbar multifidus muscle support its role as a stabilizer. *J. Biomech.* **42**, 1384–1389. (doi:10.1016/j.jbiomech.2008.09.042)
13 Hill, A. V. 1953 The mechanics of active muscle. *Proc. R. Soc. Lond. B* **141**, 104–117. (doi:10.1098/rspb.1953.0027)
14 Hill, A. V. 1938 The heat of shortening and the dynamic constants of muscle. *Proc. R. Soc. Lond. B.* **126**, 136–195. (doi:10.1098/rspb.1938.0050)
15 Lieber, R. L. & Friden, J. 2000 Functional and clinical significance of skeletal muscle architecture. *Muscle Nerve* **23**, 1647–1666. (doi:10.1002/1097-4598(200011)23:11<1647::AID-MUS1>3.0.CO;2-M)
16 Gans, C. 1982 Fiber architecture and muscle function. *Exercise Sport Sci. Rev.* **10**, 160–207.
17 Sacks, R. D. & Roy, R. R. 1982 Architecture of the hindlimb muscles of cats: functional significance. *J. Morphol.* **173**, 185–195. (doi:10.1002/jmor.1051730206)
18 Murray, W. M., Buchanan, T. S. & Delp, S. L. 2000 The isometric functional capacity of muscles that cross the elbow. *J. Biomech.* **33**, 943–952. (doi:10.1016/S0021-9290(00)00051-8)
19 Ward, S. R., Eng, C. M., Smallwood, L. H. & Lieber, R. L. 2008 Are current measurements of lower extremity muscle architecture accurate? *Clin. Orthop. Rel. Res.* **467**, 1074–1082.
20 Lieber, R. L. & Blevins, F. T. 1989 Skeletal muscle architecture of the rabbit hindlimb: functional implications of muscle design. *J. Morphol.* **199**, 93–101. (doi:10.1002/jmor.1051990108)
21 Eng, C. M., Smallwood, L. H., Rainiero, M. P., Lahey, M., Ward, S. R. & Lieber, R. L. 2008 Scaling of muscle architecture and fiber types in the rat hindlimb. *J. Exp. Biol.* **211**, 2336–2345. (doi:10.1242/jeb.017640)
22 Burkholder, T. J., Fingado, B., Baron, S. & Lieber, R. L. 1994 Relationship between muscle fiber types and sizes and muscle architectural properties in the mouse hindlimb. *J. Morphol.* **220**, 1–14. (doi:10.1002/jmor.1052200102)
23 Roy, R. R., Powell, P. L., Kanim, P. & Simpson, D. R. 1984 Architectural and histochemical analysis of the semitendinosus muscle in mice, rats, guinea pigs, and rabbits. *J. Morphol.* **181**, 155–160. (doi:10.1002/jmor.1051810204)
24 Roy, R. R., Bello, M. A., Powell, P. L. & Simpson, D. R. 1984 Architectural design and fiber type distribution of the major elbow flexors and extensors of the monkey (Cynomolgus). *J. Morphol.* **171**, 285–293.
25 Wickiewicz, T. L., Roy, R. R., Powell, P. L. & Edgerton, V. R. 1983 Muscle architecture of the human lower limb. *Clin. Orthop. Rel. Res.* **179**, 275–283.
26 Bodine, S. C., Roy, R. R., Meadows, D. A., Zernicke, R. F., Sacks, R. D., Fournier, M. & Edgerton, V. R. 1982 Architectural, histochemical, and contractile characteristics of a unique biarticular muscle: the cat semitendinosus. *J. Neurophysiol.* **48**, 192–201.
27 Winters, T. M., Takahashi, M., Lieber, R. L. & Ward, S. R. 2010 Whole muscle length-tension relationships are accurately modeled as scaled sarcomeres in rabbit hindlimb muscles. *J. Biomech.* **44**, 109–115.
28 Bang, M. L., Li, X., Littlefield, R., Bremner, S., Thor, A., Knowlton, K. U., Lieber, R. L. & Chen, J. 2006 Nebulin-deficient mice exhibit shorter thin filament lengths and reduced contractile function in skeletal muscle. *J. Cell Biol.* **173**, 905–916. (doi:10.1083/jcb.200603119)
29 Gokhin, D. S., Bang, M. L., Zhang, J., Chen, J. & Lieber, R. L. 2009 Reduced thin filament length in nebulin-knockout skeletal muscle alters isometric contractile properties. *Am. J. Physiol. Cell Physiol.* **296**, C1123–C1132. (doi:10.1152/ajpcell.00503.2008)
30 Ward, S. R. & Lieber, R. L. 2005 Density and hydration of fresh and fixed skeletal muscle. *J. Biomech.* **38**, 2317–2320. (doi:10.1016/j.jbiomech.2004.10.001)
31 Lieber, R. L. & Fridén, J. 2000 Functional and clinical significance of skeletal muscle architecture. *Muscle Nerve* **23**, 1647–1666. (doi:10.1002/1097-4598(200011)23:11<1647::AID-MUS1>3.0.CO;2-M)
32 Buchanan, T. S. 1995 Evidence that maximum muscle stress is not a constant: differences in specific tension in elbow flexors and extensors. *Med. Eng. Phys.* **17**, 529–536. (doi:10.1016/1350-4533(95)00005-8)
33 Arnold, E. M., Ward, S. R., Lieber, R. L. & Delp, S. L. 2010 A model of the lower limb for analysis of human movement. *Ann. Biomed. Eng.* **38**, 269–279. (doi:10.1007/s10439-009-9852-5)
34 Ward, S. R., Eng, C. M., Smallwood, L. H. & Lieber, R. L. 2009 Are current measurements of lower extremity muscle architecture accurate? *Clin. Orthop. Relat. Res.* **467**, 1074–1082. (doi:10.1007/s11999-008-0594-8)

35 Fukunaga, T., Kawakami, Y., Kuno, S., Funato, K. & Fukashiro, S. 1997 Muscle architecture and function in humans. *J. Biomech.* **30**, 457–463. (doi:10.1016/S0021-9290(96)00171-6)
36 Ito, M., Kawakami, Y., Ichinose, Y., Fukashiro, S. & Fukunaga, T. 1998 Nonisometric behavior of fascicles during isometric contractions of a human muscle. *J. Appl. Physiol.* **85**, 1230–1235.
37 Van Donkelaar, C. C., Kretzers, L. J., Bovendeerd, P. H., Lataster, L. M., Nicolay, K., Janssen, J. D. & Drost, M. R. 1999 Diffusion tensor imaging in biomechanical studies of skeletal muscle function. *J. Anat.* **194**, 79–88. (doi:10.1046/j.1469-7580.1999.19410079.x)
38 Heemskerk, A. M., Strijkers, G. J., Vilanova, A., Drost, M. R. & Nicolay, K. 2005 Determination of mouse skeletal muscle architecture using three-dimensional diffusion tensor imaging. *Magn. Reson. Med.* **53**, 1333–1340. (doi:10.1002/mrm.20476)
39 Lieber, R. L., Loren, G. J. & Friden, J. 1994 *In vivo* measurement of human wrist extensor muscle sarcomere length changes. *J. Neurophysiol.* **71**, 874–881.
40 Llewellyn, M. E., Barretto, R. P., Delp, S. L. & Schnitzer, M. J. 2008 Minimally invasive high-speed imaging of sarcomere contractile dynamics in mice and humans. *Nature* **454**, 784–788. (doi:10.1038/nature07104)
41 Kargo, W. J. & Rome, L. C. 2002 Functional morphology of proximal hindlimb muscles in the frog *Rana pipiens*. *J. Exp. Biol.* **205**, 1987–2004.
42 Lieber, R. L. 1997 Muscle fiber length and moment arm coordination during dorsi- and plantarflexion in the mouse hindlimb. *Acta Anat.* (*Basel*) **159**, 84–89. (doi:10.1159/000147970)
43 Alexander, R. M. 1988 *Elastic mechanisms in animal movement*. Cambridge, MA: Cambridge University Press.
44 Lieber, R. L. & Brown, C. G. 1992 Sarcomere length-joint angle relationships of seven frog hindlimb muscles. *Acta Anat.* (*Basel*) **145**, 289–295. (doi:10.1159/000147380)
45 Lieber, R. L., Ljung, B.-O. & Fridén, J. 1997 Intraoperative sarcomere measurements reveal differential musculoskeletal design of long and short wrist extensors. *J. Exp. Biol.* **200**, 19–25.
46 Lieber, R. L., Ljung, B. O. & Friden, J. 1997 Intraoperative sarcomere length measurements reveal differential design of human wrist extensor muscles. *J. Exp. Biol.* **200**, 19–25.
47 Lieber, R. L., Fazeli, B. M. & Botte, M. J. 1990 Architecture of selected wrist flexor and extensor muscles. *J. Hand Surg. Am.* **15A**, 244–250. (doi:10.1016/0363-5023(90)90103-X)
48 Loren, G. J. & Lieber, R. L. 1995 Tendon biomechanical properties enhance human wrist muscle specialization. *J. Biomech.* **28**, 791–799. (doi:10.1016/0021-9290(94)00137-S)
49 Close, R. I. 1972 Dynamic properties of mammalian skeletal muscles. *Physiol. Rev.* **52**, 129–197.
50 Brand, P. W., Beach, R. B. & Thompson, D. E. 1981 Relative tension and potential excursion of muscles in the forearm and hand. *J. Hand Surg. Am.* **3A**, 209–219.
51 Ward, S. R., Kim, C. W., Eng, C. M., Gottschalk, L. J. T., Tomiya, A., Garfin, S. R. & Lieber, R. L. 2009 Architectural analysis and intraoperative measurements demonstrate the unique design of the multifidus muscle for lumbar spine stability. *J. Bone Joint Surg. Am.* **91**, 176–185. (doi:10.2106/JBJS.G.01311)
52 Whiting, W. C., Gregor, R. J., Roy, R. R. & Edgerton, V. R. 1984 A technique for estimating mechanical work of individual muscles in the cat during treadmill locomotion. *J. Biomech.* **17**, 685–694. (doi:10.1016/0021-9290(84)90122-2)
53 Walmsley, B., Hodgson, J. A. & Burke, R. E. 1978 Forces produced by medial gastrocnemius and soleus muscles during locomotion in freely moving cats. *J. Neurophysiol.* **41**, 1203–1216.
54 Biewener, A., Konieczynski, D. & Baudinette, R. 1998 *In vivo* muscle force-length behavior during steady-speed hopping in tammar wallabies. *J. Exp. Biol.* **201**, 1681–1694.
55 Griffiths, R. I. 1987 Ultrasound transit time gives direct measurement of muscle fibre length *in vivo*. *J. Neurosci. Methods* **21**, 159–165. (doi:10.1016/0165-0270(87)90113-0)
56 Griffiths, R. I. 1989 The mechanics of the medial gastrocnemius muscle in the freely hopping wallaby (*Thylogale billardierii*). *J. Exp. Biol.* **147**, 439–456.
57 Zajac, F. E. 1989 Muscle and tendon: properties, models, scaling, and application to biomechanics and motor control. *Crit. Rev. Biomed. Eng.* **17**, 359–411.
58 Delp, S. L., Loan, J. P., Hoy, M. G., Zajac, F. E., Topp, E. L. & Rosen, J. M. 1990 An interactive graphics-based model of the lower extremity to study orthopaedic surgical procedures. *IEEE Trans. Biomed. Eng.* **37**, 757–767. (doi:10.1109/10.102791)